

An Inverse Approach to Determine the Mechanical Properties of Elastoplastic Materials Using Indentation Tests

Xiuqing Qian¹, Yanping Cao², Jianyu Zhang¹, Dierk Raabe², Zhenhan Yao³ and Binjun Fei¹

Abstract: In this work, an inverse approach based on depth-sensing instrumented indentation tests is proposed to determine the Young's modulus, yield strength and strain hardening exponent of the materials for which the elastoplastic part of the stress-strain curve can be described using a power function. Numerical verifications performed on typical engineering metals demonstrate the effectiveness of the new method. The sensitivity of the method to data noise and some experimental uncertainties are also discussed, which may provide useful information for the application of the method in practice.

Keyword: Inverse approach; mechanical properties of power law materials; indentation tests.

1 Introduction

Depth-sensing instrumented indentation tests are very attractive for probing the mechanical properties of materials at a local area and different length scales. Using the classic method proposed by Oliver and Pharr (1992), the Young's modulus and hardness of materials can be evaluated. In recent years, much effort has been made to obtain more material property information from indentation tests, e.g. the full stress-strain curves of elastoplastic materials [Giannakopoulos and Suresh (1999), Dao et al (2001), Bucaille et al (2003), Chollacoop et al (2003), Huber and Tsakmakis (1999), Cao and Lu (2004b), Cao et

al (2005, 2007), Ogasawara et al (2005)] and the properties of film-substrate interfaces [Li and Siegmund (2004)]. In order to use indentation tests to determine the material properties, the key issue is to accurately determine the correlation between the mechanical properties of materials and the indentation response. Computational modeling based on continuum mechanics e.g. using finite element method (FEM) and boundary element method (BEM) [e.g. boundary element analysis based on the solution by Han et al. (2006)], or multiscale simulations [Ma et al (2005, 2006a)] can be used to deal with this issue. The present study relies on finite element computations and starts from the comprehensive work of Dao et al (2001), in which a novel definition of the representative strain was proposed and an inverse approach constructed to determine the mechanical properties of materials. Although their inverse approach is recognized to be sensitive to data noise [Dao et al (2001), Capelhart and Cheng (2003)], the interesting definition of the representative strain [Dao et al (2001)] provides the chance to design more robust methods, such as the dual sharp indenter method [Bucaille et al (2003), Chollacoop et al (2003)] and dual or multi-depth method [Cao and Lu (2004b)]. Recently, considering the limitation of the representative strain defined by Dao et al. (2001), the authors have proposed the energy-based definition of the representative strain [Cao et al (2005)]. More recently, following the spirit in Cao et al (2005), Cao and Huber (2006) further presented several parameter-dependent definitions of the representative strain by taking the conical indenter of 70.3° as an example. The novel definitions [Cao and Huber (2006)] permit to establish approximately one-to-one relationships between the material properties (i.e., the representative stress or reduced modulus and

¹ Solid Mechanics Research Centre, Beijing University of Aeronautics and Astronautics, Beijing 100083, PR China. qianxq@buaa.edu.cn

² Max Planck Institute für Eisenforschung in Düsseldorf, 40237, Germany. cypqjl@yahoo.com or cao.y@mpie.de

³ Department of Engineering Mechanics, Tsinghua University, Beijing, 100084, PR China. demyzh@tsinghua.edu.cn

representative stress) and the directly measurable quantities in indentation tests, which basically are valid for all the elastoplastic materials for which the elastoplastic part of the stress-strain curve can be described using a power function (power law materials).

The intention of the present work is to establish a systematic inverse approach to extract the mechanical properties of power law materials from indentation tests by extending the results reported by Cao and Huber (2006) from one conical indenter to dual sharp indenter. The advantages of the present approach compared with the dual sharp indenter method in Cao et al (2005) are two fold: 1). Besides plastic properties of materials, Young's modulus can be determined by taking the effects of piling-up and sinking-in into consideration; 2). The method is applicable to a wider material range, basically to all the power law materials.

The following outline has been adopted in the present paper. Section 2 contains the material and computational models used in the present research. In section 3, the representative strains and corresponding dimensionless functions obtained in the present work are provided. The results allow us to establish an inverse approach (as shown in detail in section 4) to determine the mechanical properties of power law materials from indentation tests. In section 5, systematically numerical experiments were performed to verify the novel approach. Section 6 is a discussion of the sensitivity of the inverse approach to data noise and some experimental uncertainties frequently encountered in practice. Section 7 summarizes the main contributions made in the present research.

2 Material and computational models

Plastic behavior of many pure and alloyed engineering metals may be approximated by a power function, as shown schematically in Fig. 1. The true stress-true strain can be expressed as

$$\begin{aligned} \sigma &= E\varepsilon (\sigma \leq \sigma_y) \\ \sigma &= K\varepsilon^n (\sigma > \sigma_y) \end{aligned} \quad (1)$$

where E , K , n , σ_y and ε_y are the Young's modulus, strength coefficient, strain hardening exponent, yield stress and yield strain respectively. The total effective strain, ε , consists of two parts, i.e., the elastic strain ε_e and plastic strain ε_p . The elastoplastic part of the stress-strain curve given by equation (1) can be rewritten as

$$\sigma = \sigma_y^{1-n} (\sigma + E\varepsilon_p)^n \quad (2)$$

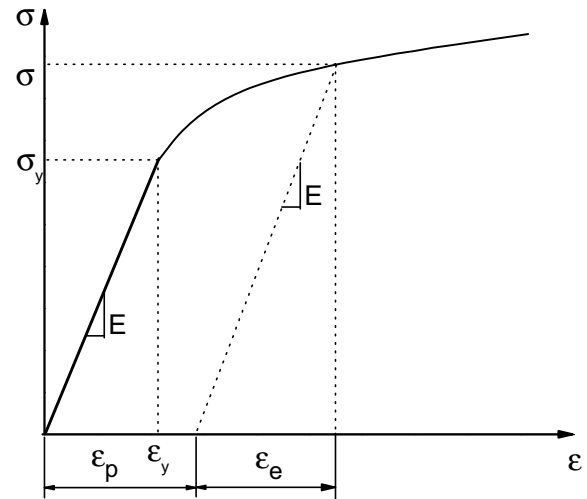


Figure 1: A schematic of power law material model

Using the concept of the indentation-response based definition of the representative strain [Cao et al (2005), Cao and Huber (2006)], the representative strain ε_r is defined as the plastic strain on the uniaxial stress strain curve (see Fig. 1) and dependent on the ratio between the reversible work W_e and the total work W_t done by the indenter (see Fig. 2).

To identify the representative strain, finite element computations were carried out using ABAQUS. In the simulation, an axisymmetric, two-dimensional model was adopted and a total of 10 000 four-node bilinear axisymmetric elements with reduced integration and hourglass control were used to model the semi-infinite solid. The boundary conditions were such that the outer surface nodes were traction-free with fixed lower surface nodes. The size of the indented solid is taken

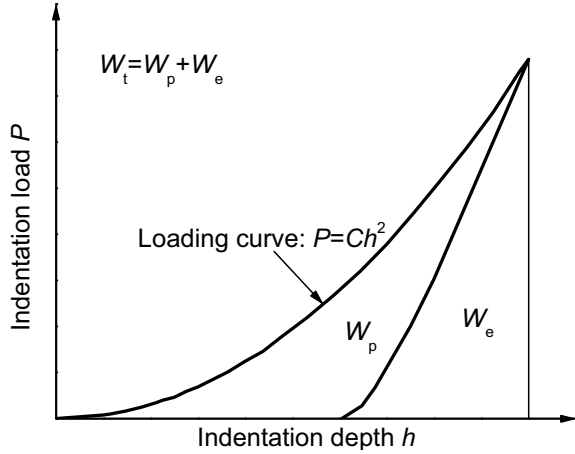


Figure 2: A schematic of the indentation loading curvature C , reversible work W_e and total work W_t

to be large enough compared with the maximum contact radius, thus the boundary conditions basically have no effect on the computational results. Dual sharp indenter with half-apex angles of 70.3° and 80° are taken. Following previous research [Cao and Huber (2006)], the indenter was assumed to be rigid. The isotropic strain hardening rule, the Von Mises yield criterion and the large deformation formulations were applied. The strain hardening exponent varies from 0 to 0.5. The ratio of Young's modulus to the yield strength E/σ_y also varies in a wide range as shown in Table 1. The material range in the present work should include basically all the power law materials.

3 Determination of representative strains and dimensionless functions

Based on the computational results and using least-squares method, the representative strains ε_r corresponding to different tip apex angles, have been identified and corresponding dimensionless functions [Cao and Huber (2006)] Π constructed. For $\theta_1 = 70.3^\circ$, the following expression of the representative strain can be identified

$$\varepsilon_{r1} = 0.05898 - \frac{0.04623}{\left(1 + e^{\frac{w_{\theta_1} - 0.15043}{0.11703}}\right)} \quad (3)$$

which leads to a one-to-one relationship between σ_{r1}/C_{θ_1} and w_{θ_1} with a high level of accuracy

given by Fig. 3, and the following equation

$$\begin{aligned} \frac{\sigma_{r1}}{C_{\theta_1}} = \Pi_{\theta_1}(w_{\theta_1}) = & 2.6888e^{\left(\frac{w_{\theta_1}}{0.10243} - 13.8155\right)} \\ & + 1.906e^{\left(\frac{w_{\theta_1}}{0.666} - 4.6052\right)} + 4.5537e^{\left(\frac{w_{\theta_1}}{0.02278} - 48.3543\right)} \\ & - 0.01032 \end{aligned} \quad (4)$$

where σ_{r1} is the representative stress corresponding to ε_{r1} , C_{θ_1} is the indentation loading curvature corresponding to the half-apex angle $\theta_1 = 70.3^\circ$, and w_{θ_1} is the ratio of reversible work to total work done by the indenter.

For the indenter of $\theta_2 = 80^\circ$, the representative strain ε_{r,θ_2} is identified as

$$\varepsilon_{r2} = 0.02602 - \frac{0.01787}{\left(1 + e^{\frac{w_{\theta_2} - 0.14648}{0.08306}}\right)} \quad (5)$$

and the corresponding one-to-one relationship between σ_{r2}/C_{θ_2} and w_{θ_2} (see Fig. 4) can be well fitted using the following equation

$$\begin{aligned} \frac{\sigma_{r2}}{C_{\theta_2}} = \Pi_{\theta_2}(w_{\theta_2}) = & -0.00299 \\ & + 2.7744e^{\left(\frac{w_{\theta_2}}{0.01573} - 69.0776\right)} + 5.8275e^{\left(\frac{w_{\theta_2}}{0.102} - 16.1181\right)} \\ & + 0.0051e^{\left(\frac{w_{\theta_2}}{0.71817}\right)} \end{aligned} \quad (6)$$

where σ_{r2} is the representative stress corresponding to ε_{r2} . The subscript " θ_2 " means that C , w and Π are corresponding to $\theta_2 = 80^\circ$.

4 An inverse approach to determine the mechanical properties of power law materials

Using the results obtained in section 3, the following inverse approach is established to determine the mechanical properties of power law materials. If Young's modulus of the indented solid is known, the strain hardening exponent n can be determined directly from the following equation

$$n = \frac{\ln\left(\frac{\sigma_{r2}}{\sigma_{r1}}\right)}{\ln\left(\frac{C_{\theta_2}}{C_{\theta_1}}\right)} \quad (7)$$

Table 1: The variation range of the ratio of E/σ_y used in the present analysis, (Poisson ratio $\nu = 0.33$)

Tip apex angle	n=0.0	n=0.1	n=0.3	n=0.5
70.3°	$(E/\sigma_y)_{\max} = 3000$	$(E/\sigma_y)_{\max} = 3500$	$(E/\sigma_y)_{\max} = 20000$	$(E/\sigma_y)_{\max} = 200000$
	$(E/\sigma_y)_{\min} = 4$	$(E/\sigma_y)_{\min} = 4.44$	$(E/\sigma_y)_{\min} = 5$	$(E/\sigma_y)_{\min} = 5$
80°	$(E/\sigma_y)_{\max} = 3000$	$(E/\sigma_y)_{\max} = 3500$	$(E/\sigma_y)_{\max} = 20000$	$(E/\sigma_y)_{\max} = 100000$
	$(E/\sigma_y)_{\min} = 6.67$	$(E/\sigma_y)_{\min} = 6.67$	$(E/\sigma_y)_{\min} = 8$	$(E/\sigma_y)_{\min} = 10$

where $\sigma_{r1} = \sigma_{r1} + E\varepsilon_{r1}$, $\sigma_{r2} = \sigma_{r2} + E\varepsilon_{r2}$, ε_{r1} , σ_{r1} , ε_{r2} and σ_{r2} are given by equations (3)–(6).

With the known n , the yield strength can be further obtained, i.e.,

$$\sigma_y = \left(\frac{\sigma_{r2}}{\sigma_{r1}^n} \right)^{\frac{1}{1-n}} \quad (8)$$

When Young's modulus of the indented solid is unknown, we suggest the following procedure to determine Young's modulus, yield strength and the strain hardening exponent of materials using the indentation response from dual sharp indenter.

First, to determine Young's modulus we invoke the interesting work of Ma et al. (2004), i.e., they proposed an interesting method to evaluate Young's modulus of materials which is given by the following simple equation

$$\frac{H_n}{E^*} = f \left(\frac{W_e}{W_t} \right) \quad (9)$$

Where H_n is the nominal hardness, E^* is reduced modulus. Subsequent studies [Ma et al (2006b), Cao et al (2006)] show that the function f in equation (9) depends the strain hardening exponent besides W_e/W_t , especially for highly plastic materials. Bearing the analysis in Ma et al (2006b) and Cao et al (2006) in mind, the relationship between the parameters C/E^* and W_e/W_t can be expressed as the following equation

$$\frac{C}{E^*} = \phi \left(\frac{W_e}{W_t}, n \right) \quad (10)$$

For $\theta_1 = 70.3^\circ$, according to the computational results in section 3, the dimensionless function ϕ in equation (10) is obtained and given as follows

$$\phi = (1 - \varphi(w_{\theta_1}))^n \psi(w_{\theta_1}) \quad (11)$$

where $\varphi(w_{\theta_1})$ can be expressed as

$$\varphi(w_{\theta_1}) = -0.0275 + 0.49115e^{\left(\frac{-w_{\theta_1}}{0.36104}\right)} \quad (12)$$

and $\psi(w_{\theta_1})$ is given by

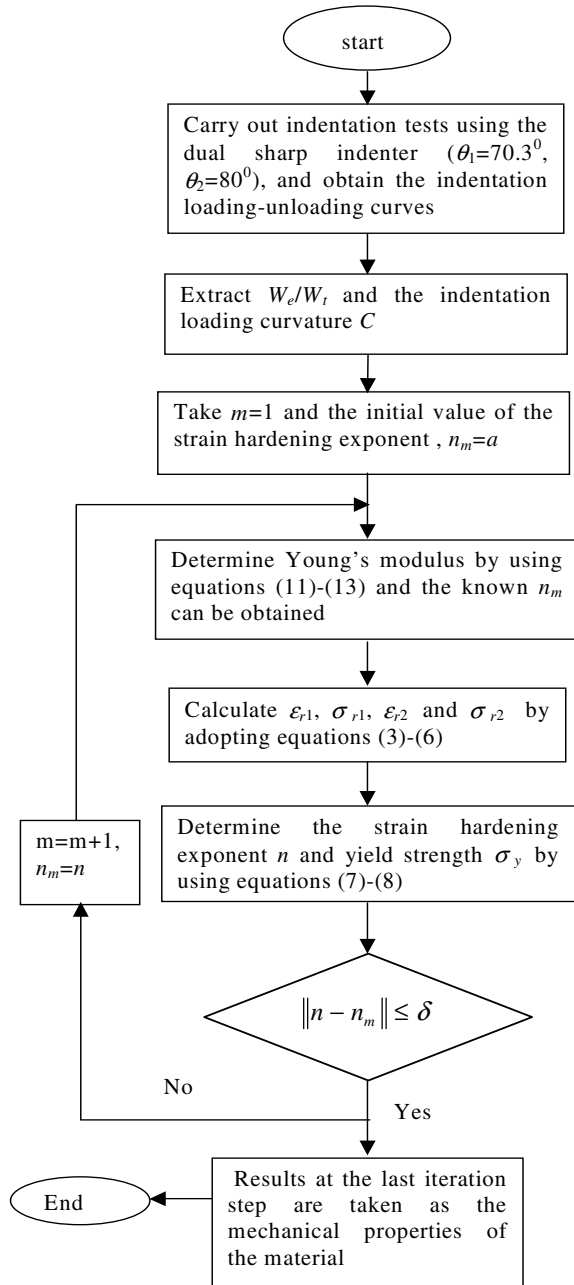
$$\begin{aligned} \psi(w_{\theta_1}) = & 4.59912w_{\theta_1} - 7.68191(w_{\theta_1})^2 \\ & + 15.55996(w_{\theta_1})^3 - 21.84057(w_{\theta_1})^4 \\ & + 15.83966(w_{\theta_1})^5 - 4.58723(w_{\theta_1})^6 \end{aligned} \quad (13)$$

Using equations (7), (8) and (11)–(13), and the results in section 3, the procedure to determine Young's modulus, yield strength and the strain hardening exponent of power law materials can be summarized as the following flow chart (Flowchart 1).

In Flowchart 1, a can be taken as a number in the range of 0~0.5, in the present algorithm, it is taken as $a=0.1$, and δ is the error tolerance, in the present work it is taken as 0.0001.

5 Numerical verification

To verify the effectiveness of the methods reported in this work, numerical verification was carried out using the properties of nine types of power law materials as listed in Table 2. Using the properties in Table 2, finite element analysis was performed; and the parameters C and $w = W_e/W_t$ obtained from FE computations were used as the inputs of the inverse approach given by Flowchart 1. The identified results are given in Table 3. A comparison of the identified results in Table 3 with the exact solutions in Table 2 shows that the novel method works very well. Here it should be pointed out that in practice the elastoplastic parts of the stress-strain curves of many metallic materials can not be exactly described using power functions. Thus, the power law description



Flowchart 1: Dual sharp indenter method to determine Young's modulus, yield strength and the strain hardening exponent of engineering materials.

is only an approximation. It should also be noted that the representative strains and the dimensionless functions are constructed in the present work for power law materials. Therefore, for the materials whose plastic behaviour significantly de-

Table 2: Material properties used to verify the representative strains and dimensionless functions proposed in the present work, $\nu=0.33$

Materials	E (GPa)	σ_y (MPa)	n
Al	70	20	0.15
Gold	79	38	0.22
Iron	180	300	0.25
Lead	16	10	0.05
Ti-6Al-4V	110	830	0.15
Silicon	107	6000	0.025
Silver	83	60	0.27
Tungsten	411	550	0.005
Titanium	120	230	0.12

Table 3: The identified elastoplastic properties of materials

Materials	E (GPa)	σ_y (MPa)	n
Al	72.0	18.8	0.16
Gold	78.0	37.0	0.23
Iron	182.5	296.3	0.25
Lead	16.2	9.33	0.07
Ti-6Al-4V	111.6	848.3	0.14
Silicon	108.2	5895	0.064
Silver	83.8	60.5	0.27
Tungsten	419.7	531.9	0.017
Titanium	120.8	213.0	0.146

viates from the power law description, the errors in the identified mechanical properties, especially the plastic properties, might be large according to our experience [Qian et al (2007)]. To highlight this issue, the following numerical experiment was carried out. First, finite element analysis was performed for the indentation into a material for which Young's modulus, $E = 120$ GPa, and the elastoplastic part of the stress-strain curve can be well fitted using a linear function instead of a power function. Second, the obtained indentation response was used as the inputs of the method given in flow chart 1. A comparison of the identified stress-strain curve with the real one is given in Fig. 5. From the figure, it can be seen that although the identified stress-strain curve fits the real one well at some points, the error between the identified yield strength and the real so-

lution is large. This big discrepancy shows the limitation of the present method (i.e., it is established based on power material model). From the present example, however it is interesting to find that the identified Young's modulus using the novel method (120.2 GPa) fits the real value (120Gpa) remarkably well, although the results in equations (10)-(13) are also obtained for power law materials.

6 Discussion on the stability of the method and the experimental uncertainties

The input data noise can not be avoided in practice. Thus, the stability of the solution to an inverse approach is very important. A lack of the stability might lead to the identified solutions using an inverse approach having nothing to do with the true solutions. For the determination of Young's modulus, the analysis on the stability of the solution can be referred to Cao et al (2006). In the present approach, the stability of the identified flow stresses is critical because they form the basis to further determine the plastic properties of materials. For $\theta_1 = 70.3^\circ$, the stability of the identified flow stresses has been examined in detail in the previous work [Cao and Huber (2006)]. For $\theta_2 = 80^\circ$, following to the analysis in Cao and Lu (2004a) and Cao and Huber (2006), the sensitivity of the solution to the errors in w is determined by using the following equation and plotted in figure 8.

$$Cond_{(w)} = \frac{w}{F_0} \left(\frac{dF_0}{dw} \right) \quad (14)$$

Using the condition number shown in Fig. 6, the sensitivity of the solution to the errors in w can be clearly identified. For the high elastic material, such as when $w \geq 0.95$, the condition number of representative stress is larger than 4.9, the stability of the identified solution is poor.

The data noise mentioned above may come from the following aspects according to the authors' experience. **1). Surface roughness.** Surface roughness is always encountered in practice, which can significantly affect the indentation response when the indentation depth is comparable with the height of the asperity [Zhang et al (2004), Herbert

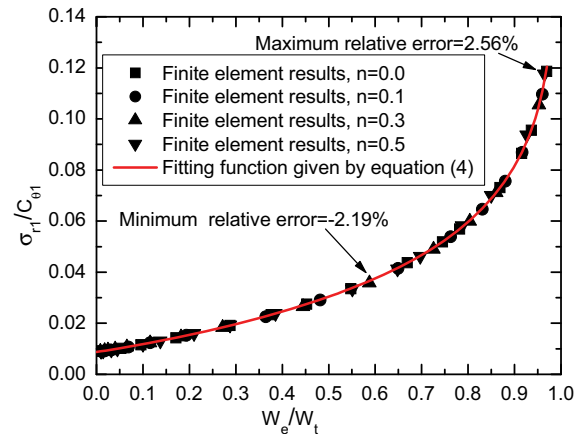


Figure 3: Relationship between σ_{r1}/C_{θ_1} and W_e/W_t

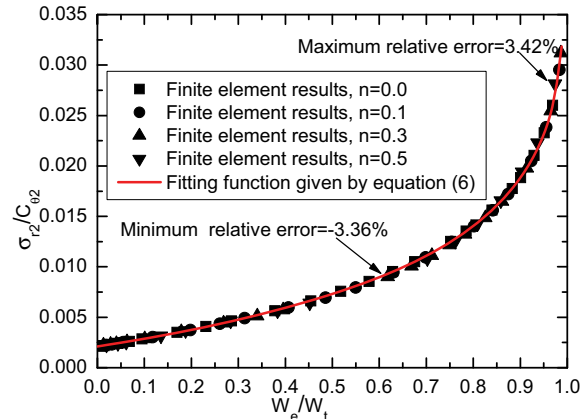


Figure 4: Relationship between σ_{r2}/C_{θ_2} and W_e/W_t

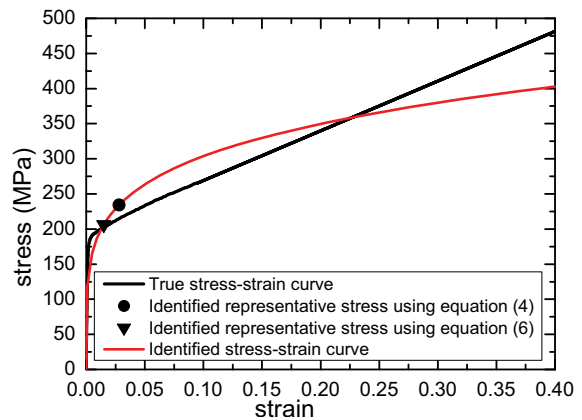


Figure 5: Comparison of the identified stress-strain curve with the real one

et al (2006), Cao et al (2007)]. **2). Tip defects.** In the simulation above, the indenter is assumed to be ideally sharp. In practice, this is not possible to achieve, and when the tip radius is not a small value compared with the indentation depth, the indentation response might significantly deviate from that corresponding to the ideally sharp indenter [Cheng and Cheng (1998)]. **3). Surface layer.** In the preparation of the samples, a surface layer might be produced whose properties can be apparently different from the bulk [Bucaille et al (2004)]. **4). Geometrically necessary dislocations (GNDs).** GNDs-induced indentation size effect has been widely investigated [Nix and Gao (1998), Begley and Hutchinson (1998), Elmustafa et al (2000), Chen et al (2002)]. It is shown that when the indentation depth is at micron or sub-micron, the effect of GNDs on the indentation loading curve can be very significant [Cao and Lu (2005)]. **5). Surface energy.** Zhang and Xu (2002) have systematically investigated the effect of surface work and reported that it could lead to depth-dependent indentation hardness. In this case the indentation loading curvature may also be depth-dependent due to the surface work. In order to make the errors from above sources negligible, the indentation depth should be much larger than the height of the asperity for the rough surface, tip radius of a non-ideally sharp indenter, thickness of the surface layer and the material characteristic length corresponding to GNDs. The indentation depth should also be much larger than the critical depth in order to overcome the effect of surface work according to Zhang and Xu (2002).

7 Conclusions

Base on the concept of the indentation response-based definition of the representative strain [Cao et al (2005), Cao and Huber (2006)], simple and explicit expressions of the relationship between the material properties and the directly measurable quantities from indentation tests are obtained for dual sharp indenter. Using these relations, an inverse approach to extract Young's modulus, yield strength and the strain hardening exponent of materials using dual sharp indenter is proposed.

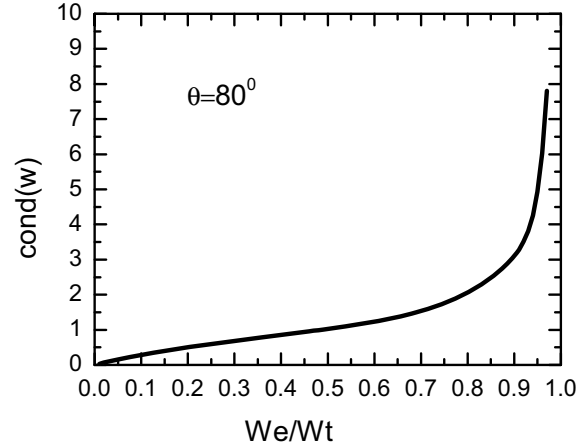


Figure 6: A plot of the condition number

The performance of the method is carefully verified by numerical experiments. The results show that for power law materials, the present method can provide a very good estimation on the mechanical properties. But it should be noted that the power law model is just an approximation and in practice the complexity of the materials [Ma et al. (2006c), Zaafarani et al. (2006)] might lead to a macroscopic stress-strain curve far from the power law description. We have highlighted that the identified plastic properties might contain significant errors in the case that the plastic behaviour of a material significantly deviates from the power law description. However, it is interesting to find from the present numerical example, that the identified Young's modulus using the present method is reliable even the elastoplastic part the stress-strain curve of the material can not be well fitted using a power function. Further systematic investigation of this interesting finding is necessary and important and will be performed in the near future. Stability of the inverse approach and the experimental uncertainties are also discussed which provides useful information for the application of the method in practice.

Acknowledgement: YPC acknowledges the financial support from Alexander von Humboldt Foundation in Germany.

References

- Begley, M. R.; Hutchinson, J. W.** (1998): The mechanics of size-dependent indentation. *J. Mech. Phys Solids*, vol. 46(10), pp. 2049-2068.
- Bucaille, J. L.; Stauss, S.; Felder, E.; Michler, J.** (2003): Determination of plastic properties of metals by instrumented indentation using different sharp indenters. *Acta Mater.*, vol. 51(6), pp. 1663-1678.
- Bucaille, J. L.; Rossoll, A.; Moser, B.; Stauss, S.; Michler, J.** (2004): Determination of the matrix in situ flow stress of a continuous fibre reinforced metal matrix composite using instrumented indentation. *Materials Science and Engineering A*, vol. 369(1-2), pp. 82-92.
- Cao, Y. P.; Lu, J.** (2004a): Depth-sensing instrumented indentation with dual sharp indenters: stability analysis and corresponding regularization schemes. *Acta Mater.*, vol. 52(5), pp. 1143-1153.
- Cao, Y. P.; Lu, J.** (2004b): A new method to extract the plastic properties of metal materials from an instrumented spherical indentation loading curve. *Acta Mater.*, vol. 52(13), pp. 4023-4032.
- Cao, Y. P.; Qian, X. Q.; Lu, J.; Yao, Z. H.** (2005): An energy-based method to exact plastic properties of metal materials from conical indentation tests. *J Mater Res.*, vol. 20(5), pp. 1194-1206.
- Cao, Y. P.; Lu, J.** (2005): Size-dependent sharp indentation. I - A closed form expression of the indentation loading curve, *J. Mech. Phys Solids*, vol. 53(1), pp. 33-48.
- Cao, Y. P.; Huber, N.** (2006): A further investigation on the definition of the representative strain in conical indentation. *J Mater Res.*, vol. 21(7), pp. 1810-1821.
- Cao, Y. P.; Qian, X. Q.; Lu, J.** (2006): On the determination of reduced Young's modulus and hardness of elastoplastic materials using a single sharp indenter. *J Mater. Res.*, vol. 21(1), pp. 215-224.
- Cao, Y. P.; Qian, X. Q.; Huber, N.** (2007): Spherical indentation into elastoplastic materials: indentation-response based definitions of the representative strain. *Materials Science & Engineering A*, vol. 454, pp. 1-13.
- Capehart, T. W.; Cheng, Y. T.** (2003): Determining constitutive models from conical indentation: Sensitivity analysis. *J Mater Res.*, vol. 18(4), pp. 827-832.
- Chen, J.; Yuan, H.; Wittmann, F. H.** (2002): Computational Simulations of micro-indentation tests using gradient plasticity. *CMES-CMES: Computer Modeling in Engineering & Sciences*, vol. 3(6), pp. 743-754.
- Cheng, Y. T.; Cheng, C. M.** (1998): Further analysis of indentation loading curves: Effects of tip rounding on mechanical property measurements. *J Mater Res.*, vol. 13 (4), pp. 1059-1064.
- Chollacoop, N.; Dao, M.; Suresh, S.** (2003): Depth-sensing instrumented indentation with dual sharp indenters. *Acta Mater.*, vol. 51(13), pp. 3713-3729.
- Dao, M.; Chollacoop, N.; Van Vliet, K. J.; Venkatesh, T. A.; Suresh, S.** (2001): Computational modeling of the forward and reverse problems in instrumented sharp indentation. *Acta Mater.*, vol. 49(19), pp. 3899-3918.
- Elmustafa, A. A.; Eastman, J. A.; Rittner, M. N.; Weertman, J. R.; Stone, D. S.** (2000): Indentation size effect: large grained aluminum versus nanocrystalline aluminum-zirconium alloys. *Scripta Materialia*, vol. 43(10), pp. 951-955.
- Giannakopoulos, A. E.; Suresh, S.** (1999): Determination of elastoplastic properties by instrumented sharp indentation. *Scripta Mater.*, vol. 40(10), pp. 1191-1198.
- Han, F., Pan, E., Roy, A. K. et al.** (2006): Responses of piezoelectric, transversely isotropic, functionally graded, and multilayered half spaces to uniform circular surface loadings. *CMES: Computer Modeling in Engineering & Sciences* Vol. 14, pp.15-29.
- Herbert, E. G.; Oliver, W. C.; Pharr, G. M.** (2006): On the measurement of yield strength by spherical indentation. *Philosophical Magazine*, vol. 86, pp. 5521-5539.
- Huber, N.; Tsakmakis, C.** (1999): Determination of constitutive properties from spherical in-

dentation data using neural networks. Part. I: the case of pure kinematic hardening in plasticity laws, Part. II: Plasticity with nonlinear isotropic and kinematic hardening. *J Mech Phys Solids*, vol. 47, pp. 1569-1607.

Li, W.; Siegmund, T. (2004): Numerical study of indentation delamination of strongly bonded films by use of a cohesive zone model. *CMES: Computer Modeling in Engineering & Sciences*, vol. 5 (1), pp. 81-90.

Ma, D. J.; Ong, Ch. W.; Wong, S. F. (2004): New relationship between Young's modulus and nonideally sharp indentation parameters. *J. Mater. Res.*, vol. 19(7), pp. 2144-2151.

Ma, D. J.; Zhang, T. H.; Ong, Ch. W. (2006a): Evaluation of the effectiveness of representative methods for determining Young's modulus and hardness from instrumented indentation data. *J Mater Res.*, vol. 21(1), pp. 225-233.

Ma, J.; Lu, H.; Wang, B. et al. (2005): Multi-scale simulations using generalized interpolation material point (GIMP) method and SAMRAI parallel processing. *CMES: Computer Modeling in Engineering & Sciences*, vol. 8 (2) pp. 135-152.

Ma, J.; Liu, Y.; Lu, H. B. et al. (2006b): Multiscale simulation of nanoindentation using the generalized interpolation material point (GIMP) method, dislocation dynamics (DD) and molecular dynamics (MD). *CMES: Computer Modeling in Engineering & Sciences*, vol. 16 (1), pp. 41-55.

Ma, A.; Roters F.; Raabe, D. (2006c): A dislocation density based constitutive model for crystal plasticity FEM including geometrically necessary dislocations. *Acta Materialia*, vol. 54, pp. 2169-2179.

Nix, W. D.; Gao, H. (1998): Indentation size effects in crystalline materials: a law for strain gradient plasticity. *J Mech Phys Solids*, vol. 46(3), pp. 411-425.

Ogasawara, N.; Chiba, N.; Chen, X. (2005): Representative strain of indentation analysis, *J Mater Res.*, vol. 20(8), pp. 2225-2234.

Oliver, W. C.; Pharr G. M. (1992): An improved technique for determine hardness and elastic modulus using load and displacement sensing indentation experiments. *J. Mater. Res.*, vol. 7(6),

pp. 1564-1583.

Qian, X. Q.; Cao, Y. P.; Lu, J. (2007): Dependence of the representative strain on the hardening functions of metallic materials in indentation. *Scripta Materialia*, vol. 57, pp. 57-60.

Zaafarani, N.; Raabe, D.; Singh R. N.; Roters, F.; Zaefferer, S. (2006): Three-dimensional investigation of the texture and microstructure below a nanoindentation in a Cu single crystal using 3D EBSD and crystal plasticity finite element simulations. *Acta Mater.* vol. 54, pp. 1863-1876.

Zhang, T. Y.; Xu, W. H. (2002): Surface effects on nanoindentation. *J. Mater. Res.*, vol. 17, pp. 1715-1720.

Zhang, T. Y.; Xu, W. H.; Zhao, M. H. (2004): The role of plastic deformation of rough surfaces in the size-dependent hardness. *Acta Mater.*, vol. 52, pp. 57-68.

